IMPROVING ACCURACY AND EXPLAINABILITY OF ONLINE HANDWRITING RECOGNITION

Anonymous authors
Paper under double-blind review

ABSTRACT

Handwriting recognition technology allows recognizing a written text from a given data. The recognition task can target letters, symbols, or words, and the input data can be a digital image or recorded by various sensors. A wide range of applications from signature verification to electronic document processing can be realized by implementing efficient and accurate handwriting recognition algorithms. Over the years, there has been an increasing interest in experimenting with different types of technology to collect handwriting data, create datasets, and develop algorithms to recognize characters and symbols. More recently, the OnHW-chars dataset has been published that contains multivariate time series data of the English alphabet collected using a ballpoint pen fitted with sensors. The authors of OnHW-chars also provided some baseline results through their machine learning (ML) and deep learning (DL) classifiers.

In this paper, we develop handwriting recognition models on the OnHW-chars dataset and improve the accuracy of previous models. More specifically, our ML models provide 11.3%-23.56% improvements over the previous ML models, and our optimized DL models with ensemble learning provide 3.08%-7.01% improvements over the previous DL models. In addition to our accuracy improvements over the spectrum, we aim to provide some level of explainability for our models to provide more logic behind chosen methods and why the models make sense for the data type in the dataset. Our source codes, data, and models will be made publicly available for verifiability and reproducibility of our results.

1 INTRODUCTION

1.1 PROBLEM STATEMENT AND RELATED WORK

Handwriting is defined to be the writing characteristics of an individual Priya et al. (2016). Handwriting recognition is the process of converting written text (whether that be letters, numbers, words, symbols, etc.) into a form which can be interpreted and recognized by a computer. One major goal in handwriting recognition analysis involves a computer interpreting letters or words that have been written by hand. Handwriting data can be interpreted by a machine (computer) in two distinct categories: online and offline.

Offline handwriting recognition tries to recognize a handwritten text from its static digital image that has been produced at the time of writing. Online handwriting data is captured at run time, by some sort of sensor. This sensor can be in the pen used, such as in Ott et al. (2020) or through the device it was captured on a tablet or digitizer, as in LaViola & Zeleznik (2007). The sensor records spatio-temporal signals in the form of a multivariate time series throughout the process. This provides a large advantage for online handwriting over offline for certain applications or implementations. Recording characters through a sensor, as opposed to digital images, as is in online handwriting recognition, has the added benefit of capturing more information. The sensor captures additional pieces of information such as the time it takes to write, cadence, and unique stylizations in the way it is written, all of which may not be able to be captured by a static image. These dynamic readings can produce more favourable results in certain applications as there is more information to be obtained. Applications such as signature verification Fahmy (2010) and e-security or e-health Faundez-Zanuy et al. (2020) can make use of online handwriting recognition particularly well.

Over the years, there has been an increasing interest to experiment with different types of technology to collect handwriting data, to create datasets, and to develop algorithms to perform recognition of characters and symbols Alpaydin (1997); Wang & Chuang (2012); Guyon et al. (1994). More recently, the OnHW-chars dataset Ott et al. (2020) has been published that contains multivariate time series data of the English alphabet collected using a ballpoint pen fitted with sensors. The pen used to collect this data was the STABILO DigiPen, which is fitted with various sensors: 2 accelerometers, 1 gyroscopes, 1 magnetometers and a force sensor. Each letter in OnHW-chars is an $n \times 14$ vector, where n is the amount of timesteps collected. For each timestep, 14 features were collected as follows: for each of the two accelerometers, gyroscopes and magnetometers, x, y and z values were collected, as well as one feature representing time and the final feature is a binary value of whether or not force was applied with the pen on the paper. The dataset OnHW-chars provides a basis to develop algorithms to correctly identify which letter is being written based on sensor data. While publishing a dataset, the authors of Ott et al. (2020) also provided some baseline results through their machine learning (ML) and deep learning (DL) classifiers. DL classifiers, trained on the same dataset OnHW-chars, have later been improved in a more recent paper Ott et al. (2022a). In addition, Ott et al. (2022a) reports on the accuracy of classifiers trained on other new datasets, such as OnHW-equations, OnHW-symbols and OnHW-words. There have been a sequence of other papers published, exploring other topics and models, such as in Ott et al. (2022b;c;d); Klaß et al. (2022), however we will focus on Ott et al. (2020; 2022a) as these are the most accurate reported results. To our knowledge, source codes of algorithms and models used in Ott et al. (2022a) have not been released to public yet.

A brief description of OnHW-chars Being the most recent and publicly available online handwriting dataset with some state-of-the-art classifiers trained on it, we focus on developing classifiers for OnHW-chars. OnHW-chars contains multiple versions of each letter from a to z, collected from 119 unique users. Left handed writers were excluded from the dataset.

There is a separate dataset for lowercase and uppercase letters as well as a combined dataset of both lowercase and uppercase letters. Additionally, the data was pre-split in Ott et al. (2020) into 5 folds of train and test split for each of the lowercase, uppercase and combined datasets. For each of these, a writer independent (WI) and a writer dependent (WD) version of the split is provided in Ott et al. (2020). In WI, writer sets of the train and the test split of a fold are disjoint. If a writer appears in the training (test) data, they are not in the test (train). However, in WD, a writer's data will be split between the training and test data. All in all, this gives 6 datasets (3 cases and 2 writer dependency) further split into 5 folds each. In all this yields 30 datasets. When reporting on the accuracy of OnHW-chars classifiers in Ott et al. (2020; 2022a), they average over 5 folds. Thus, they present classifier accuracies on 6 datasets, which we denote by lowercase-WD (L-WD), lowercase-WI (L-WI), uppercase-WD (U-WD), uppercase-WI (U-WI), combined-WD (C-WD), combined-WI (C-WI).

1.2 Contributions

Our contributions in this paper are twofold:

Improving on the accuracy of classifiers on OnHW-chars To our knowledge, the best accuracy results of ML classifiers and DL classifiers for the OnHW-chars dataset are the ones reported in Ott et al. (2020) and Ott et al. (2022a), respectively. As mentioned before, Ott et al. (2022a) improves DL classifiers in Ott et al. (2020). Our ML and DL models yield, respectively, 11.3%-23.56% and 2.17%-4.34% improvements over the accuracy of the best ML and DL models reported in Ott et al. (2020; 2022a). We obtain these improvements thanks to the use of state-of-the-art feature extraction algorithms and optimizations of the models. We further utilize the ensemble learning method to achieve 3.08%-7.01% improvements over the best results reported in Ott et al. (2020; 2022a). We refer the reader to Table 2 for a summary of our results, and to Sections 3 and 4 for more details about the models and workflows used. Additionally, we refer the reader to the Figure 4 for an overview of our workflow.

Providing verifiable and reproducible results with some level of explainability In addition to providing improvements to accuracy across the spectrum, this paper aims to provide some level of explainability of these models so as to provide more logic as to why these methods are chosen and

why the models make sense for the type of data in the dataset. In addition to prediction accuracy, it is important to assess ML models on how they come to their decisions Fauvel et al. (2020). One goal is to explain the reason as to why it makes sense to use the models used for the specific data at hand. For the DL models we extend the local interpretable model-agnostic explanations (LIME) Ribeiro et al. (2016) architecture to add explainability to our multivariable time series (MTS) data. We refer the reader to Sections 4 and 5 for more details.

Finally, we would like to add some transparency to the process. Along with the paper, a public repository will be provided containing all the preprocessing and code for each model, so that it is reproducible and verifiable. Some models, specifically some DL models contain a level of randomness, which will alter the results slightly from one run of the model to the next. For these situations, a loadable encoded representation of the model will be provided as well. With this, we would like to make the model generation process public, so that others can have access to these models, as well as verify, reproduce, and improve our results.

2 PROCESSING THE ONHW-CHARS DATASET

2.1 PREPROCESSING AND FILTERING

The OnHW-chars dataset is provided publicly in its raw form. In Ott et al. (2020), detailed explanations are provided for preprocessing OnHW-chars. However, to our knowledge, the pre-processed versions are not publicly available, which introduces some challenge for reproducing results and providing fair comparisons. According to Ott et al. (2020), a high pass filter is applied to the data with a cutoff frequency of 1 (Hz) to remove the gravitational acceleration from the accelerometer recordings. Also, a moving filter with a window of size 11 is used and that acts as a low pass filter, allowing high-frequency noise removal from the data. It is noted in Ott et al. (2020) that the filtering is used when applying ML models and only trimming is applied for the DL models. Our pre-processing steps on raw data also vary depending on the choice of the classification algorithm. We will provide the details of changes in pre-processing steps for each methodology.

Table 1: Statistical characteristics of the OnHW-chars dataset subsets in terms of mean (μ) and standard deviation (σ) of the total number of timestamps for each sample of data.

Subset	μ	σ
Lowercase (L)	44.05	29.93
Uppercase (U)	52.85	42.82
Combined (C)	48.45	37.20

As mentioned before in Section 1, OnHW-chars contains 6 datasets: L-WD, L-WI, U-WD, U-WI, U-WD, C-WD, and C-WI with different characteristics. Table 1 presents statistical characteristics of the OnHW-chars subsets in terms of mean (μ) and standard deviation (σ) of the total number of samples for each instance of data. The σ for each subset in relation to their respected μ indicates that the number of samples for each instance in OnHW-chars is notably spread out and confirms the presence of outliers. In order to reduce the impact of outliers on the data and make the data more coherent, we discard instances based on the statistical characteristics of the lowercase subset. This is because only between 2%–4% of normal English literature characters are written in capitals depending on the text and the genre. Therefore, considering real-life applications in practice, the lowercase subset can be a better candidate for detecting and removing outliers. Using μ and σ of the lowercase subset as given in Table 1, we remove any data sample with sequence length more than $\mu + 2\sigma \approx 104$. Considering that $\mu - 2\sigma$ yields a negative value, we determine, based on inspecting the dataset, that any sequence of length less than 10 should be discarded.

2.2 EXTRACTING STATISTICAL FEATURES FROM ONHW-CHARS

The OnHW-chars contains variable length time-series data points. On the other hand, ML algorithms commonly accept fixed length data points for their training. Therefore, for each variable-length data point in OnHW-chars, we are motivated to extract a fixed number of features that carry as much information as possible about the data.

We first pre-process OnHW-chars as mentioned in Section 2.1, which is then provided as input to the tsfresh software package Christ et al. (2018). Tsfresh is the main component used in our feature extraction process. Tsfresh applies the feature extraction and scalable hypothesis testing (FRESH) algorithm Christ et al. (2016) to extract features from variable length time series data, and further selects (and filters) relevant features based on their significance to the classification task at hand Christ et al. (2018). It computes a total of 794 time series features, obtained from the combination of 63 different time series characterization methods. The features range from simple statistical features such as the mean, and standard deviation to more complex ones including Fourier coefficients.

After applying tsfresh's feature extraction algorithm to OnHW-chars, there were a total of 10231 features extracted for every letter recording. This comes as a result of 787 features extraction per dimension for the 13-dimensional OnHW-chars dataset. These features are then further filtered using tsfresh's feature selection step, which conducts a series of scalable hypothesis tests and significantly drops the number of features. For example, 1571 features are extracted from the first fold of L-WI in the OnHW-chars dataset. We should emphasize that, in order to control leakage of information from the test set, we applied the feature selection step only on the training set. Once we have the selected features from the training set, those same features are directly extracted from the test set. The reader can find a flowchart depicting this in the in Figure 5.

In our experiments, we observe that accuracy of ML classifiers is significantly affected by the choice of the parameter n_significant in tsfresh. The parameter n_significant represents the number of classes a feature should be able to predict. In the case of classifying lowercase or uppercase letters, each feature we select should be able to predict any of the 26 classes. This is where the trade off comes in. When selecting n_significant to be high, only a very small set of features will be selected. This tends to lead to low classification accuracy due to the high amount of information loss. Counter to that, when selecting n_significant to be low, we get many features but they may not predict the majority of class labels. This trade off is later visualized in Figure 6. Through experimentation with the k-nearest neighbors (kNN) model, we chose to use n_significant $= 17$ in our feature extraction step. We note that this choice may not be optimal and a better choice may exist. Once feature extraction and selection steps are completed, we use the extracted features to train our ML models. During training, other transformations may be applied to data, which we explain in the following.

3 Developing models on the OnHW-chars dataset

3.1 Machine learning (ML) algorithms

For developing ML models, we follow two strategies. In both strategies, the OnHW-chars dataset is preprocessed and filtered as described in Section 2.1. In our first strategy, we extract fixed-length features from the preprocessed and filtered OnHW-chars dataset, as explained in Section 2.2, and that these features are provided as input to the training of ML models, where we use Decision Tree, Random Forest, Extra Trees, Logistic Regression, k-Nearest Neighbours, and Support Vector Machines. In our second strategy, we investigate elastic similarity measures for classification, by using the preprocessed and filtered OnHW-chars for training kNN using Dynamic Time Warping (DTW). In Section C.1, we provide details about our ML models, and we refer the reader to Table 2 for our results and a comparison with the results from Ott et al. (2020). In particular, we obtain 11.3%-23.56% improvements over the ML models in Ott et al. (2020).

3.2 Deep learning (DL) algorithms

In order to provide a comparison with the (baseline) results in Ott et al. (2020; 2022a), we first train DL models considered in Ott et al. (2020; 2022a) using the software package tsai Oguiza (2020) Our trained models include fully convolutional network (FCN), residual neural network (ResNet), long short-term memory (LSTM), bidirectional LSTM (BiLSTM), inception time (InceptionTime), xception time (XceptionTime), and explainable convolutional neural network (CNN) for multivariate time series (XCM). We explain each DL methodology that we train on OnHW-chars in Section C.2. We refer the reader to Table 2 for our results and a comparison with the best of the results from Ott et al. (2020; 2022a). Our baseline models yield 2.17%-3.91% improvements over the DL models in Ott et al. (2020; 2022a). Our DL models have been developed using the software package tsai

Table 2: A summary of our results in comparison with Ott et al. (2020; 2022a). Columns labeled with "OnHW" show the best of best results from Table 4 in Ott et al. (2020) and Table 6 in Ott et al. (2022a). Values in bold font indicate the best result of their column in their group in the table. Values in bold font that are also underlined indicate the best result in their groups in the table. There are 5 groups: ML Baseline, DL Baseline, DL Optimized, Ensemble Learning, and Best Overall.

		Lowercase				Uppercase				Combined			
		WD		WI		WD		WI		WD		WI	
		Proposed	OnHW	Proposed	OnHW	Proposed	OnHW	Proposed	OnHW	Proposed	OnHW	Proposed	OnHW
ML Baseline	5NN with NCA	77	-	68.35	-	81.51	-	74.72	-	64.96	-	55.73	-
	5NN with PCA	57.7	-	44.42	-	59.49	-	48.7	-	36.1	-	23.5	-
	DT	49.34	30.49	44.85	22.89	55.91	33.23	51.48	24.32	37.39	20.32	33.06	20.33
	ET	70.49	-	61.81	-	73.83	-	66.15	-	56.8	-	48.2	-
	KNN-DTW	65.41	-	54.62	-	72.08	-	62.72	-	50.69	-	41.14	-
	LogReg	71.98	56.16	66.54	49.6	77.36	62.59	73.55	**53.26**	60.68	43.95	54.87	41.66
	RFC	71.45	58.02	64.97	45.55	75.32	63.19	69.25	45.96	58.33	43.6	51.65	43.62
	Linear SVM	75.64	**62.09**	68.1	**51.8**	80.75	**70.61**	74.67	54	66.24	**48.77**	58.04	**46.56**
	RBF SVM	**78.42**	-	**71.08**	-	**81.91**	-	**76.82**	-	**66.89**	-	**59.87**	-
	KNN	67.61	49.17	55.96	34.09	70.29	57.49	61.42	36.68	50.33	38.3	39.57	33.08
ML Improvements		16.33		19.28		11.3		23.56		18.12		13.31	
DL Baseline	FCN	86.93	81.62	73.67	71.48	88.16	85.37	78.71	77.24	77.39	67.41	62.15	58
	InceptionTime	**92.74**	84.14	**83.44**	75.28	**94.54**	87.8	**88.43**	81.62	83.17	70.43	70.49	61.68
	BiLSTM-FCN	86.53	-	73.74	-	88.11	-	79.54	-	77.89	-	63.31	-
	LSTM-FCN	86.5	81.43	74.36	71.41	88.28	85.43	79.91	77.07	77.92	67.34	63.26	57.93
	LSTM	88.33	79.83	78.33	73.03	90.83	88.68	84.59	81.91	79.15	67.83	67.61	60.29
	BiLSTM	88.69	82.43	78.5	75.72	91.3	89.15	84.37	81.09	79.42	69.37	67.5	63.38
	(Bi)MLSTM-FCN	86.7	-	74.49	-	89.2	-	80.74	-	79.15	-	65.1	-
	MLSTM-FCN	86.63	80.21	74.15	71.9	89.16	85.25	80.89	77.44	79.12	69.33	64.82	60.14
	ResCNN	90.23	82.52	78.26	72	91.53	86.91	82.41	78.64	80.22	67.55	65.43	58.67
	ResNet	92.48	83.01	81.64	71.93	94.11	86.41	86.28	78.03	82.84	68.56	68.65	58.74
	XCM	81.94	74.39	72.36	68.12	84.11	81.67	76.41	74.32	70.99	58.18	61.82	51.99
	XceptionTime	91.95	81.41	82.86	70.76	94.02	85.94	87.93	78.23	**83.32**	66.7	**71.8**	56.92
	CNN-BiLSTM	-	**89.66**	-	**80**	-	**92.58**	-	**85.64**	-	**78.98**	-	**68.44**
DL Optimized	InceptionTime	**92.79**	-	**83.91**	-	**94.75**	-	**88.74**	-	**82.71**	-	**71.82**	-
	LSTM-FCN	85.27	-	75.87	-	89.44	-	81.82	-	77.72	-	65.8	-
	LSTM	89.49	-	80.86	-	91.32	-	85.26	-	79.16	-	70.51	-
	MLSTM-FCN	87.35	-	76.36	-	87.35	-	80.65	-	79.19	-	67.83	-
DL Improvements		3.13		3.91		2.17		3.1		4.34		3.38	
Ensemble Learning	Plurality (top 3)	93.47	-	84.95	-	94.98	-	89.27	-	85.08	-	74.13	-
	Soft (top 2 + opt.)	93.66	-	85.39	-	95.14	-	89.74	-	85.36	-	74.56	-
	Weighted Soft	**94.18**	-	**86.12**	-	**95.66**	-	**90.34**	-	**85.99**	-	**74.8**	-
	Soft (all)	93.34	-	84.52	-	94.76	-	89.01	-	85.49	-	73.77	-
Best Overall		**94.18**	**89.66**	**86.12**	**80**	**95.66**	**92.58**	**90.34**	**85.64**	**85.99**	**78.98**	**74.8**	**68.44**
Overall Improvements		4.52		6.12		3.08		4.7		7.01		6.36	

Oguiza (2020), where we used the default architectural parameters as in tsai Oguiza (2020) while setting the epoch number to 50 and the learning rate to 0.001.

4 OPTIMIZATIONS

In the following sections, we discuss architectural parameter and hyperparameter optimization of some of our DL models and also the use of ensemble learning to further improve the accuracy of our DL models. Even though we observed similar accuracy after parameter optimizations, the use of ensemble learning provided up to 2.98% improvements over our DL models, whence 3.08%-7.01% improvements over the results reported in Ott et al. (2020; 2022a); see Table 2. For DL baseline methods in Ott et al. (2020; 2022a), as indicated in Table 2, CNN-BiLSTM had the best performance among all other DL models. However, we could not implement the same model due to the lack of detailed information about CNN architecture, such as the total number of layers, the total number of filters in each layer, and filter sizes. CNN, as a class of artificial neural networks, can take different structures leading to different performances and dramatically affecting the results for comparison purposes. Nevertheless, compared to CNN-BiLSTM, our InceptionTime implementation had a better performance overall.

4.1 OPTIMIZING ACRHITECTURAL PARAMETERS AND HYPERPARAMETERS

Since the InceptionTime model did better overall among our base DL models, we decided to optimize it. Due to a large choice of architectural parameters in LSTM, we also decided to optimize LSTM, LSTM-FCN, and MLSTM-FCN. Of course, other models could be optimized but we leave this for future work. We used the optuna framework Akiba et al. (2019) with 100 number of trials in our study. Across all of the optimization studies, our search space for the "learning rate" is set

between 0.00001 and 0.01 with logarithmic increments and the "epoch number" is exhausted from 25 to 100 with increments of 25. In our study, search space for InceptionTime parameters are as follows: "nf" takes $4, 8, 16, 32, 40, 48, 56, 64, 128$; "depth" takes values from 1 to 15 with increments of 1 and "fc_dropout" takes values from 0 to 0.9 with increments of 0.1 The search space for LSTM parameters are as follows: "n_layers" takes values from 1 to 5 with increments of 1; "rnn_dropout" and "fc_dropout" take values from 0 to 0.9 with increments of 0.1; "bidirectional" takes True or False. The search space for LSTM-FCN and MLSTM-FCN parameters are as follows: "rnn_layers" takes values from 1 to 5 with increments of 1; "rnn_dropout" and "fc_dropout" takes values from 0 to 0.9 with increments of 0.1; "bidirectional" takes True or False. We first optimized the model parameters independently on the L-WI, U-WI, and C-WI datasets. We used the same parameter sets when training our models on the respective WD datasets. Therefore, for a small number of cases, our models trained on WD underperform in comparison with the base DL models, where the most significant drop is observed for MLSTM-FCN trained on the U-WD dataset. One could ideally optimize the parameters independently on WD as well, but we do not pursue this path mainly because of the high cost of optimizing parameters and the minor performance gains due to parameter optimization over our base models (e.g. compare the accuracy of InceptionTime in Table 2 for DL Baseline vs. DL Optimized). More details, including the optimized models and their parameters will be publically available and the accuracy of the optimized results are presented in Table 2. Our optimization efforts resulted in similar accuracy in comparison with our base DL models.

4.2 Optimizing via the use of ensemble learning

While the models above outperform the previously best published results and the optimizations of these models yield even more accurate results, we wanted to find a way to increase the accuracy even more. We begin by analyzing how the models make predictions and specifically, how each model differs from each other when making predictions. We look at the data where (the best) models make incorrect predictions and see how other models perform in these points. This analysis leads us to believe that combining the predictions of these models, in an ensemble method, may be able to help lead us to increased accuracy Dietterich (2000). We present the findings of our analysis, as well as results below.

4.2.1 Failure space

We will define the failure space of a classification model as the space of input data where the model makes an incorrect predictive classification. We examined how the failure spaces of each of the 16 models trained above (12 base models and the 4 optimized models), compared to one another. It was hypothesized that given the different architectures and even parameters (on a small scale) would cause different models to fail in different places. In other words, the intersection of the failure spaces of these models does not fully overlap. If this were to be the case, then there would be reason to believe that the models may be focusing on different aspects of the MTS and that there is potential for a combination of models to be used to collectively produce an output. Below, are two seperate analyses, exploring the failure spaces of the 16 models.

First, we explore how each of the models perform in comparison to one another. The dataset is fixed to the C-WI, fold 0 dataset. We then fix a letter, say "Z" and examine all test data points that are actually "Z"s. For each piece of test data, we determine whether each model predicted it correctly or incorrectly. The results are displayed in a heatmap in Figure 1. Each row corresponds to the prediction of a different model, and each column corresponds to a unique test data. The colour represents a correct or incorrect prediction, with a correct prediction being white and an incorrect prediction being black. We call this type of an analysis the prediction space analysis. We notice that the map looks very spotted. There are a few columns that are all black, but there are also many columns that are split between correct and incorrect predictions. This tells us that there may be a use to combining these models in such a way to diminish the incorrect predictions. The prediction space analysis shows us that oftentimes, when even the best performing models are incorrect, other models may predict the data point correctly.

After examining the failure spaces of each of the models, it was found that the models were failing in different places. What this means is that for a given test case, a portion of the 16 models can fail, but oftentimes others will succeed. From here we hypothesized that there may exist some combination of models, which can work together to make predictions more accurately than individual models.

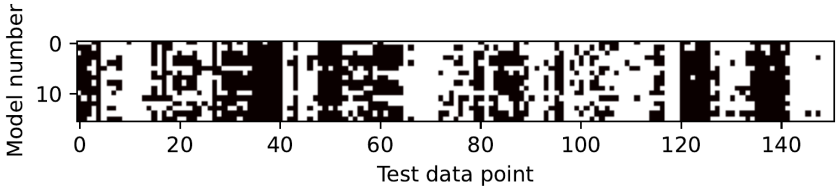

Figure 1: The prediction space analysis in the both independent fold 0 dataset. The models are numbered as follows: 0:XceptionTime,1:InceptionTime, 2: ResNet, 3: LSTM FCN, 4: BiLSTM FCN, 5:LSTM, 6:BiLSTM, 7:MLSTM FCN, 8:BiMLSTM FCN, 9:FCN, 10:ResCNN, 11:XCM, 12: Optimized InceptionTime, 13: Optimized LSTM, 14: Optimized LSTM FCN, 15:Optimized MLSTM FCN.

4.2.2 PLURALITY VOTING

Through our failure space analysis, we wanted to try to find a way to combine multiple models to make one single prediction. The first attempt at this is plurality voting, where each model will make a prediction on a piece of data and vote on the predicted class. The final output class is the class which receives the most votes Zhou (2012). A tie in plurality voting is broken arbitrarily. This method produced results slightly worse than our best performing models. This however is not unexpected since the best models and worst models all have an equal say in the output. One way to resolve this will be weighted voting and will be explored in the section below. Another resolution is to drop the poorly performing models and only consider the top tier (best 3 models) for the plurality voting. This resulted in an increase of up to 1% on the best performing algorithm for each dataset.

4.2.3 WEIGHTED VOTING

In cases where the individual classifiers are of unequal performance, it can be valuable to give more voting power to the stronger performing models and less voting power to the weaker models Zhou (2012). As can be seen in Table 2, we trained 16 models with varying levels of performance and accuracy. In the Plurality voting method, the top 4 best models were considered in the voting process for the best results. For better accuracy, we tried to include more models in a weighted voting method, with lower weights. The models were divided into 3 categories: top, middle, and bottom tier. Out of the 16 models considered, 4 belonged in the top tier (InceptionTime, Optimized InceptionTime, XceptionTime and ResNet), 4 in the middle tier (ResCNN, Optimized LSTM, Optimized MLSTM_FCN and Optimized LSTM_FCN) and 8 in the bottom tier (LSTM, BILSTM, MLSTM_FCN, BIMLSTM_FCN, FCN, BILSTM_FCN, LSTM_FCN,XCM). The weights were established so that the top tier models are considered first and lower tier models are considered only in the events of a tie. The bottom tier of models get a weight of 1 applied to their vote, the middle tier gets a weight of 9 applied to their vote and the top tier gets a weight of 45 applied to their vote. If all 4 bottom tier models agree on a class, their vote is still outweighed by a single middle tier model. Similarly, if all middle tier models agree on a class, their vote is outweighed by a single top tier model.

4.2.4 SOFT VOTING

The models trained above provide a probability that a given input belongs to each of the letter classes. The class with the highest probability becomes the predicted class from the model and up until now is all that has been considered. In soft voting, for each class, the probabilities of each prediction class are averaged. The class with the highest average is outputted. Soft voting was implemented, with an improvement on both plurality voting and weighted voting.

4.2.5 WEIGHTED SOFT VOTING

The strongest approach we have found is the weighted soft voting model. This combines the benefits of soft voting, with those of weighted voting. Provided here is a soft model, that gives weights to the probabilities depending on the quality of model. This model, using the same weights asabove was the best performing of the ensemble methods tried and yielded between a 0.91% and 2.98% increase

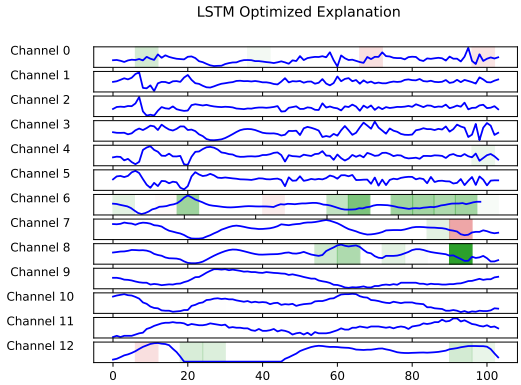

Figure 2: Explanation of LSTM Optimized on the both independent fold 0 dataset, for a test letter "B". Blue lines represent 13-dimensional data with respect to time.

4.2.6 Ensemble learning in practice

As seen above in Table 2, the accuracy of the ensemble learning techniques are competitive with or improved upon existing methods. An increase in accuracy when using ensemble methods is consistent with the literature Yang (2011); Yerima et al. (2015); Raza (2019); Li et al. (2017). However, we should explore the impact of implementing a protocol like this in a practical application.

It is important to examine the accuracy vs. training-time trade-off Wasay et al. (2020); Yang (2011) of using ensemble learning models. Not only do ensemble learning models take longer to train, but they are also larger in size and require more time to infer predictions. The size of the ensemble learning model and time it takes to run are both combinations of the models used to build them, plus some small overhead. The time required to make an inference and the size of the models must both be considered when using ensemble models in practice. We hypothesize that user-device based prediction may not be practical with ensemble methods. To use ensemble methods, it may be useful or even required to use server-based predictions as the models can be housed on a server with sufficient storage and computing power.

5 Further explaining DL models

It is important to not treat these DL models as black box, but to gain some intuition as to why predictions are being made in these ways. We already provided some explanations regarding failure spaces of the models, which motivated the use of ensemble learning. In this section, we use an interpretation of LIME Ribeiro et al. (2016) for time series data, lime-for-timeMetzenthin (2020). In this interpretation, the time series is divided into 20 "slices" and the importance of each slice is determined by the LIME algorithm. Additionally, since we are working with MTS data, each of the 13 signals (channels) will be analyzed separately. The top 30 signals and slices, in terms of importance, will be examined. A green bar, indicating a score greater than 0, represents that this section of the data has a positive impact on the model output and a red bar, indicating a score less than 0, represents that this section of the data has a negative impact on the model output. The graphs below show all 13 channels of the raw data with an importance bar overlayed on top of it. The darkness of colour indicates how much influence that slice of the data has on the classification.

We show two examples of this explanation analysis, to give some backing and explanation as to the predictions being made. The first is an example of where a model predicts correctly and is fairly certain about its prediction. This is shown in Figure 2 regarding the explanation of the Optimized LSTM model correctly predicting a letter "B" in the C-WI fold 0 dataset. As we can see, the green and red bars are primarily on the 6th, 8th and 12th channel. This means that these channels have more influence (or importance) on the overall prediction. Each channel corresponds to a signal from a sensor and thus different dimension of the MTS.

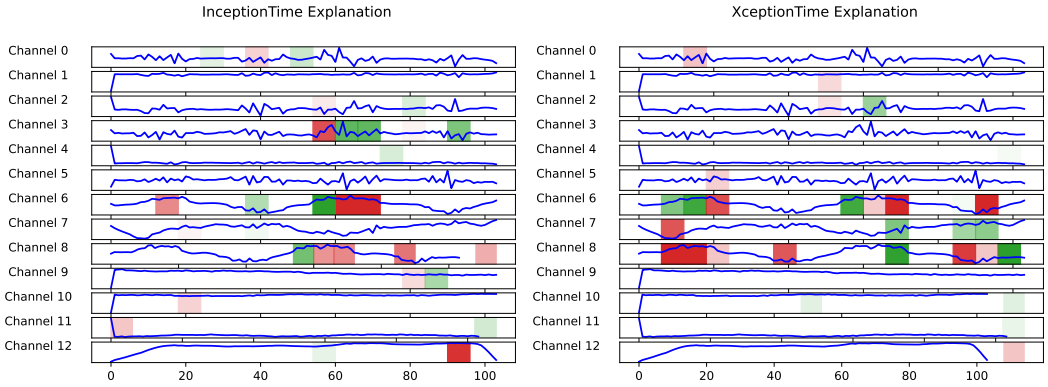

Figure 3: The first image on the left is the explanation of a correct InceptionTime prediction of the letter "M". The second image on the right is the explanation of an incorrect XceptionTime prediction of the same letter. XceptionTime predicts "A". Blue lines represent 13-dimensional data with respect to time.

The second example we show the explanation of two different (yet both strong) models, which disagree about the output class. This is shown in Figure 3. As we can see both of these models inherit influence from different places. One example of this is that XceptionTime puts influence into the first channel for this prediction whereas InceptionTime does not, while InceptionTime puts influence into the 4th channel and XceptionTime does not. Additionally, we see different sections of the 6th, 8th and 12th channels being highlighted. What this tells us is that not only are different models making different predictions from each other, but they are deriving importance from different parts of the MTS. This leads us to believe that by combining these models, we may be able to take advantage of different models inheriting importance from different areas, thus improving the overall "catchment" of the models chosen. Along with the failure space analysis, showing that the 16 models fail in different places, these explanations show that the models also value different parts of the signal to have different levels of importance. These two pieces of analysis provide even more motivation on the previous section on ensemble learning, as this provides reason to believe that there may be potential in combining these models to produce a signal output, with better success than any individual model.

6 Concluding Remarks

We developed various handwriting recognition models on the OnHW-chars dataset Ott et al. (2020). Our ML models improved the accuracy of the previously known ML models Ott et al. (2020) up to 23.56% and our DL models (coupled with ensemble methods) improved the accuracy of the previously known DL models Ott et al. (2022a) up to 7.01%. We also provided some level of explainability for our models. Our explanations motivated the use of ensemble learning to boost the accuracy of our models and justified its success. Our results can be reproduced and verified via our source code which will be made public. Being the most recent and publicly available online handwriting dataset with some state-of-the-art classifiers trained on it, we have chosen to develop our models on the OnHW-chars dataset. We expect that our techniques would be applicable to other datasets in a more general context.

An interesting future work would be to develop better ensemble methods. For example, one could try to optimize the weights in the voting stage using meta learners or combinatorial approaches Cruz et al. (2014). Another approach would be to consider Bayesian model averaging Monteith et al. (2011). Finally, it would be interesting to run a deeper analysis on the explainability of models, and to understand the importance of features as this would provide some insight to improve the performance and efficiency of the models.

REFERENCES

T. Akiba, S. Sano, T. Yanase, T. Ohta, and M. Koyama. Optuna: A Next-generation Hyperparameter Optimization Framework. In *KDD'19: Proceedings of the 25rd ACM SIGKDD International Conference on Knowledge Discovery and Data Mining*, pp. 2623–2631, 2019.

E. Alpaydin. Combining Multiple Representations and Classifiers for Pen-based Handwritten Digit Recognition. *Proceedings of the Fourth International Conference on Document Analysis and Recognition*, pp. 637–640, 1997.

J. Caiado, N. Crato, and D. Pena. Comparison of Times Series with Unequal Length in the Frequency Domain. *Communications in Statistics - Simulation and Computation*, 38(3):527–540, 2009.

M. Christ, A. W. Kempa-Liehr, and M. Feindt. Distributed and Parallel Time Series Feature Extraction for Industrial Big Data Applications. *Asian Machine Learning Conference. Workshop on Learning on Big Data*, 2016. https://arxiv.org/abs/1610.07717v1.

M. Christ, N. Braun, J. Neuffer, and A. W. Kempa-Liehr. Time Series Feature Extraction on Basis of Scalable Hypothesis Tests (tsfresh - A Python Package). *Neurocomputing*, 307:72–77, 2018.

R. Cruz, R. Sabourin, and G. Cavalcanti. On meta-learning for dynamic ensemble selection. In *2014 22nd International Conference on Pattern Recognition*, pp. 1230–1235. IEEE, 2014.

T. Dietterich. Ensemble Methods in Machine Learning. *MCS 2000: Multiple Classifier Systems - First International Workshop*, 1857:1–15, 2000.

M. Fahmy. Online Handwritten Signature Verification System based on DWT Features Extraction and Neural Network Classification. *Ain Shams Engineering Journal*, 1(1):59–70, 2010.

M. Faundez-Zanuy, J. Fierrez, M. Ferrer, M. Diaz, R. Tolosana, and R. Plamondon. Handwriting Biometrics: Applications and Future Trends in e-security and e-health. *Cognitive Computation*, 12(5):940–953, 2020.

K. Fauvel, T. Lin, V. Masson, È. Fromont, and A. Termier. XCM: An Explainable Convolutional Neural Network for Multivariate Time Series Classification, 2020. https://arxiv.org/abs/2009.04796.

H.I Fawaz, B. Lucas, G. Forestier, C. Pelletier, D.F. Schmidt, J. Weber, G.I. Webb, L. Idoumghar, P. Muller, and F. Petitjean. InceptionTime: Finding AlexNet for Time Series Classification. *Data Mining and Knowledge Discovery*, 34(6):1936–1962, 2020.

P. Geurts, D. Ernst, and L. Wehenkel. Extremely Randomized Trees. *Machine Learning*, 63(1): 3–42, 2006.

A. Graves and J. Schmidhuber. Framewise Phoneme Classification with Bidirectional LSTM Networks. *Proceedings of IEEE International Joint Conference on Neural Networks, 2005*, 4:2047–2052, 2005.

I. Guyon, L. Schomaker, R. Plamondon, M. Liberman, and S. Janet. UNIPEN Project of Online Data Exchange and Recognizer Benchmarks. *Proceedings of the 12th IAPR International Conference on Pattern Recognition*, 2:29–33, 1994.

S. Hochreiter and J. Schmidhuber. Long Short-Term Memory. *Neural Computation*, 9(8):1735–1780, 1997. ISSN 0899-7667. doi: 10.1162/neco.1997.9.8.1735.

F. Karim, S. Majumdar, H. Darabi, and S. Chen. LSTM Fully Convolutional Networks for Time Series Classification. *IEEE Access*, 6:1662–1669, 2018.

F. Karim, S. Majumdar, H. Darabi, and S. Harford. Multivariate LSTM-FCNs for Time Series Classification. *Neural Networks*, 116:237–245, 2019.

E. Keogh and C. Ratanamahatana. Exact Indexing of Dynamic Time Warping. *Knowledge and Information Systems*, 7(3):358–386, 2005. https://doi.org/10.1007/s10115-004-0154-9.

A. Klaß, S. Lorenz, M. Lauer-Schmaltz, D. Rügamer, B. Bischl, C. Mutschler, and F. Ott. Uncertainty-aware evaluation of time-series classification for online handwriting recognition with domain shift, 2022. URL https://arxiv.org/abs/2206.08640.

J. LaViola and R. Zeleznik. A Practical Approach for Writer-Dependent Symbol Recognition Using a Writer-Independent Symbol Recognizer. *IEEE Transactions on Pattern Analysis and Machine Intelligence*, 29(11):1917–1926, 2007.

J. Li, N. Song, G. Yang, M. Li, and Q. Cai. Improving Positioning Accuracy of Vehicular Navigation System During GPS Outages Utilizing Ensemble Learning Algorithm. *Information Fusion*, 35: 1–10, 2017.

E. Metzenthin. LIME For Time, 2020. https://github.com/emanuel-metzenthin/Lime-For-Time.

K. Monteith, J. Carroll, K. Seppi, and T. Martinez. Turning bayesian model averaging into bayesian model combination. In *The 2011 International Joint Conference on Neural Networks*, pp. 2657–2663, 2011. doi: 10.1109/IJCNN.2011.6033566.

I. Oguiza. tsai - A State-of-the-art Deep Learning Library for Time Series and Sequential Data, 2020. https://github.com/timeseriesAI/tsai.

F. Ott, M. Wehbi, T. Hamann, J. Barth, B. M. Eskofier, and C. Mutschler. The OnHW Dataset: Online Handwriting Recognition from IMU-Enhanced Ballpoint Pens with Machine Learning. *Proceedings of the ACM on Interactive, Mobile, Wearable and Ubiquitous Technologies*, 4(3): 1–20, 2020.

F. Ott, D. Rügamer, L. Heublein, T. Hamann, J. Barth, B. Bischl, and C. Mutschler. Benchmarking Online Sequence-to-Sequence and Character-based Handwriting Recognition from IMU-Enhanced Pens. *International Journal on Document Analysis and Recognition (IJDAR)*, pp. 1433–2825, 2022a. doi: 10.1007/s10032-022-00415-6. https://arxiv.org/abs/2202.07036.

F. Ott, D. Rügamer, L. Heublein, B. Bischl, and C. Mutschler. Joint classification and trajectory regression of online handwriting using a multi-task learning approach. In *2022 IEEE/CVF Winter Conference on Applications of Computer Vision (WACV)*, pp. 1244–1254, 2022b. doi: 10.1109/WACV51458.2022.00131.

F. Ott, D. Rügamer, L. Heublein, B. Bischl, and C. Mutschler. Domain adaptation for time-series classification to mitigate covariate shift, 2022c. URL https://arxiv.org/abs/2204.03342.

F. Ott, D. Rügamer, L. Heublein, B. Bischl, and C. Mutschler. Cross-modal common representation learning with triplet loss functions, 2022d. URL https://arxiv.org/abs/2202.07901.

F. Pedregosa, G. Varoquaux, A. Gramfort, V. Michel, B. Thirion, O. Grisel, M. Blondel, P. Prettenhofer, R. Weiss, V. Dubourg, J. Vanderplas, A. Passos, D. Cournapeau, M. Brucher, M. Perrot, and E. Duchesnay. Scikit-learn: Machine Learning in Python. *Journal of Machine Learning Research*, 12:2825–2830, 2011.

A. Priya, S. Mishra, S. Raj, S. Mandal, and S. Datta. Online and Offline Character Recognition: A Survey. In *2016 International Conference on Communication and Signal Processing (ICCSP)*, pp. 0967–0970, 2016.

E. Rahimian, S. Zabihi, S.F. Atashzar, A. Asif, and A. Mohammadi. XceptionTime: A Novel Deep Architecture based on Depthwise Separable Convolutions for Hand Gesture Classification, 2019. http://arxiv.org/abs/1911.03803.

K. Raza. Chapter 8 - Improving the Prediction Accuracy of Heart Disease with Ensemble Learning and Majority Voting Rule. In *U-Healthcare Monitoring Systems*, Advances in Ubiquitous Sensing Applications for Healthcare, pp. 179–196. Academic Press, 2019.

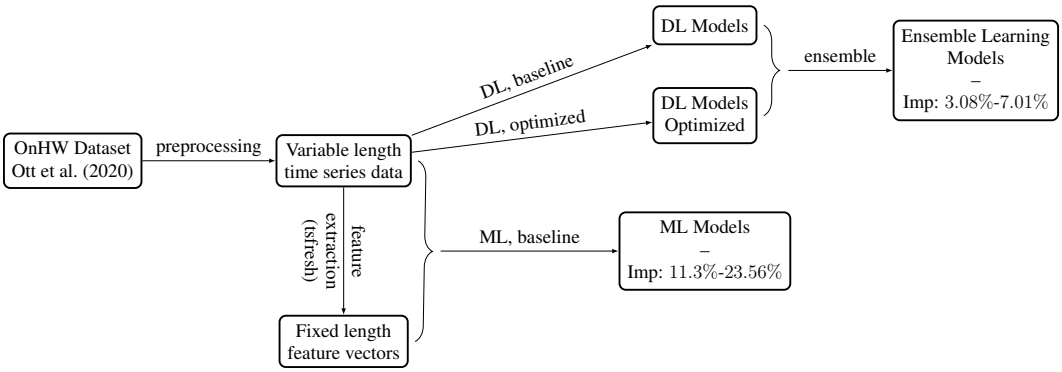

Figure 4: Our workflow for training machine learning (ML) and deep learning (DL) models, and utilizing the ensemble method. Feature extraction is performed using tsfresh Christ et al. (2018). Average accuracy improvements (Imp) are reported with respect to the previous ML and DL models in Ott et al. (2020; 2022a).

M. Ribeiro, S. Singh, and C. Guestrin. "Why Should I Trust You?": Explaining the Predictions of any Classifier. *Proceedings of the Demonstrations Session, NAACL HLT 2016, The 2016 Conference of the North American Chapter of the Association for Computational Linguistics: Human Language Technologies*, pp. 97–101, 2016.

S. Seto, W. Zhang, and Y. Zhou. Multivariate Time Series Classification Using Dynamic Time Warping Template Selection for Human Activity Recognition, 2015. `https://arxiv.org/abs/1512.06747`.

J. Wang and F. Chuang. An Accelerometer-based Digital Pen with a Trajectory Recognition Algorithm for Handwritten Digit and Gesture Recognition. *IEEE Transactions on Industrial Electronics*, 59(7):2998–3007, 2012.

Z. Wang, W. Yan, and T. Oates. Time Series Classification from Scratch with Deep Neural Networks: A Strong Baseline, 2016. `http://arxiv.org/abs/1611.06455`.

A. Wasay, B. Hentschel, Y. Liao, S. Chen, and S. Idreos. MotherNets: Rapid Deep Ensemble Learning. *Proceedings of Machine Learning and Systems*, 2: 199–215, 2020. `https://proceedings.mlsys.org/paper/2020/file/3ef815416f775098fe977004015c6193-Paper.pdf`.

K. Weinberger and L. Saul. Distance Metric Learning for Large Margin Nearest Neighbor Classification. *Journal of Machine Learning Research*, 10(2):207–244, 2009.

L. Yang. Classifiers Selection for Ensemble Learning based on Accuracy and Diversity. *Procedia Engineering*, 15:4266–4270, 2011.

S. Yerima, S. Sezer, and I. Muttik. High Accuracy Android Malware Detection Using Ensemble Learning. *IET Information Security*, 9(6):313–320, 2015.

Z. Zhou. *Ensemble Methods: Foundations and Algorithms*. Chapman and Hall/CRC, 2012.

X. Zou, Z. Wang, Q. Li, and W. Sheng. Integration of Residual Network and Convolutional Neural Network along with Various Activation Functions and Global Pooling for Time Series Classification. *Neurocomputing*, 367:39–45, 2019.

A Appendix - Work Flowchart

Included in Figure 4, is a chart describing the workflow of how our framework.

B APPENNDIX - TSFRESH FLOWCHART

Included in Figure 5 is a flowchart describing the feature extraction process through tsfresh.

Figure 5: Feature extraction flowchart.

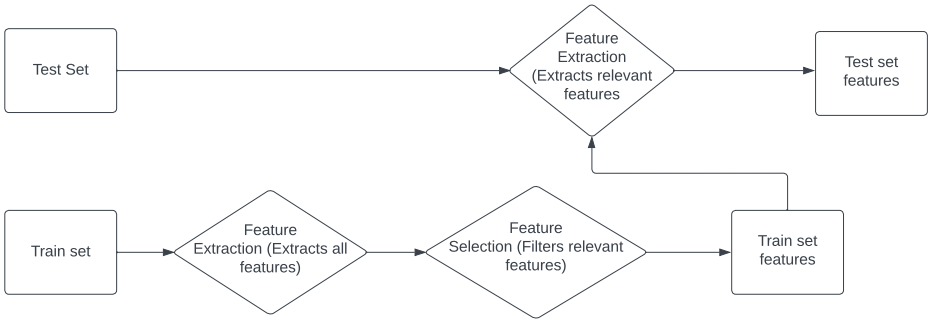

C APPENDIX - MODELS TRAINED

C.1 MACHINE LEARNING ALGORITHMS

C.1.1 STRATEGY 1: ML MODELS TRAINED ON FIXED-LENGTH FEATURE VECTORS

As explained in Section 2.2, we utilize tsfresh Christ et al. (2018) to extract fixed-length feature vectors, which are then used as input in training some ML models. To our knowledge this is the first instance in which tsfresh has been applied to the OnHW-chars dataset. In order to provide a fair comparison with the accuracy results as reported in Table 4 in Ott et al. (2020), we train Random Forest, Decision Tree, Logistic Regression, Linear Support Vector Machines, and k-Nearest Neighbor algorithms. To further improve accuracy, we implement metric learning as described in Weinberger & Saul (2009) for kNN. Additionally, we train the Extra-Trees classifier implemented using scikit-learn Pedregosa et al. (2011), based off of Geurts et al. (2006), and SVM with non-linear kernels. Our implementation mainly uses the software package scikit-learn Pedregosa et al. (2011). In the following, we provide an overview and explanation for each algorithm we implement following Strategy 1.

Decision tree: Decision Trees are tree-like structures where each branch represents a test on a feature, and the leaf nodes represent classes. Starting at the root node, we perform a sequence of tests to move along the tree. The prediction is based on the leaf node we end up on. To establish a baseline comparison with the results in Ott et al. (2020), we use decision trees with default parameters as in scikit-learn Pedregosa et al. (2011), and no additional preproccessing is applied on the extracted feature set.

Random forest: Random Forests are a collection of individual decision trees. This collection operates together as an ensemble where each tree gets a vote for the end label/class. The class with the most votes is the one that is chosen in the end. As before, we would like a baseline comparison with Ott et al. (2020) to outline the effects tsfresh had on the end classification accuracy. We choose scikit-learn's default parameters: 100 trees, no defined max depth, minimal sample split of 2, and minimal samples leaf of 1.

Extra trees: Extra Trees outlined in Geurts et al. (2006) is implemented in scikit-learn Pedregosa et al. (2011), and they are similar to a Random Forests with a few key differences. These are not implemented in Ott et al. (2020). We implement them with the default parameters of scikit-learn,

similiar to the above mentioned models. This gives us 100 trees, no defined maximum depth, a minimum sample split of 2 and no specified max leaf nodes.

Logistic regression: Logistic Regression is also a baseline we would like to establish to further outline the effects tsfresh has on the end classification accuracy. First the QuantileTransformer Pedregosa et al. (2011) is fitted to the selected feature set with 1000 quantiles and a uniform output distribution. After fitting the transformer it is applied to both the test and train sets to scale each of the features. When running logistic regression we choose default parameters as in scikit-learn Pedregosa et al. (2011), except that we changed the default maximum iterations parameter from 100 to 1000.

kNN: kNN is a simple non-parametric algorithm which classifies new observations based on the distance from known observations. We use scikit-learn's default parameter $k = 5$ to show the impact of our feature extraction method in comparison with the one in Ott et al. (2020). Using the selected features from Section 2.2, we scale the feature set using QuantileTransformer Pedregosa et al. (2011) in the same way we did previously for logistic regression. No dimensionality reduction is performed. To find an appropriate level of n_significant, we construct a series of models with varying levels of n_significant, as seen in Figure 6. Here we take n_significant $= 17$ for the feature selection step of all our models. We note that this choice may not be optimal and a better choice may exist.

Supervised metric learning with kNN: As an extension to the previously mentioned kNN algorithm, we apply metric learning in a supervised fashion to improve accuracy scores. The pipeline remains identical, but instead of using QuantileTransformer, neighborhood component analysis (NCA) from scikit-learn Pedregosa et al. (2011) is implemented to learn a distance metric and reduce the dimensionality of the test and train sets. NCA improves kNN accuracy by directly maximizing the stochastic variant of the leave-one-out kNN score on the training set. When in use, NCA requires standardized data, so StandardScalar Pedregosa et al. (2011) was first applied to the selected features. For NCA, we specify the parameters "init = LDA", so that LDA (i.e., linear discriminant analysis) is used to initialize the linear transformation, and "n_components $= 20$", reducing the inputted feature space down to 20 features. This choice of n_components is obtained from the accuracy of kNN models over different levels of n_components, as seen in Figure 7.

SVM: Similiar to kNN, SVM aims to group observations based on their distance from known groups. QuantileTransformer is applied to the feature set in the same fashion as we used it before. When running SVM, we used the same parameters as in Ott et al. (2020). Furthermore, we implement SVM with both a linear and Gaussian kernel.

C.1.2 Strategy 2: ML models trained on variable-length time series data

As opposed to some ML models that receive fixed-length feature vectors as input, some ML models can directly work with variable length time-series data. In our second strategy, we train dynamic time warping (DTW) models based on the preprocessed and filtered OnHW-chars dataset as explained in Section 2.1.

DTW: DTW is a technique to measure the optimal alignment between 2 time series. Keogh & Ratanamahatana (2005). One main advantage to using DTW as a similarity measure, as opposed to Euclidean distance, is that DTW supports vectors of differing lengths. One downside to DTW, however, is that it is not a distance metric as it does not satisfy the triangle inequality and it is not positive definite Keogh & Ratanamahatana (2005). Despite this, it is still often used to measure (or approximate) the distance between two time series. DTW has grown in use for time series data clustering Seto et al. (2015).

Having support for differing length vectors is important for time series data and particularly crucial for sensor data such as the OnHW-chars dataset Ott et al. (2020), since these vectors will often have different lengths. One approach is to zero-pad the time series and determine the distance between these zero-padded vectors using Euclidean distance, however Euclidean distance compares the points in each vector in sequence Caiado et al. (2009). This is problematic for the OnHW-chars dataset because the actual length it takes to write each letter is inconsistent and slight inconsistencies in the timing will massively affect the similarity and particularly problematic when there are large

Figure 6: kNN accuracy with various levels of n_significant, using lowercase writer-independent (L-WI) data.

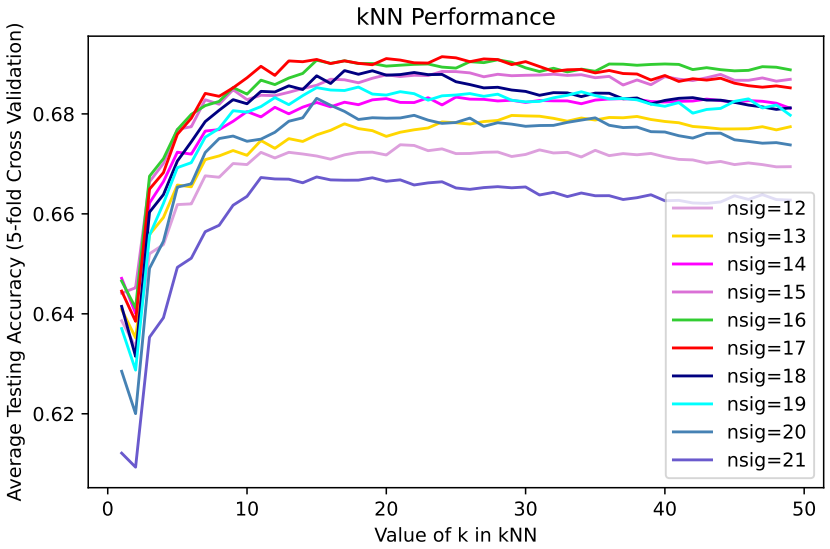

Figure 7: kNN accuracy over various levels of n_components, using lowercase writer-independent (L-WI) data.

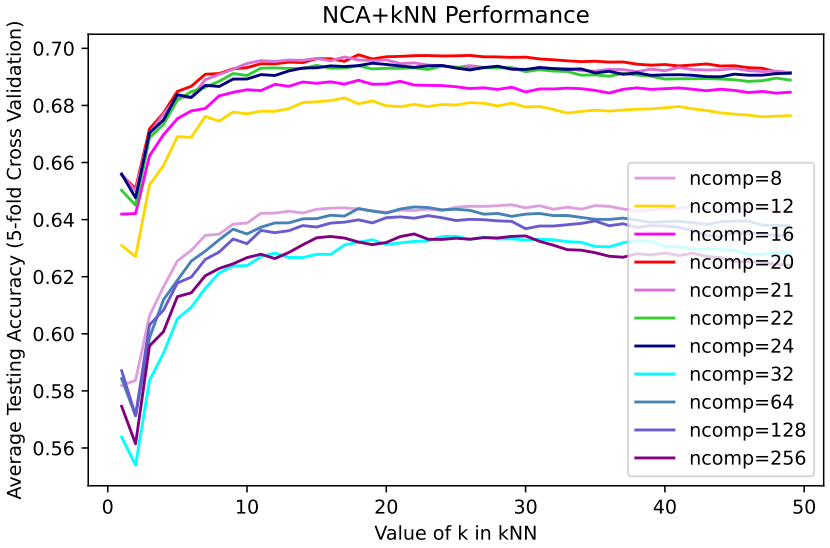

differences in lengths. Variable length can also be attributed to issues with the sensor. Similarity measures which are flexible to variable length vectors, such as DTW, are preferred in this case. For our purposes, these similarity measures will be used in a kNN algorithm to classify the vectors.

C.2 Deep Learning Algorithms

FCN: FCN has been shown to achieve state-of-the-art performance on the task of classifying time series sequences Wang et al. (2016). The basic block of FCN is a convolutional layer followed by a batch normalization layer and a ReLU activation layer. The final network is built by stacking three convolution blocks. Like ResNet, the FCN architecture excludes pooling operations to prevent overfitting Wang et al. (2016). In order to improve generalization, batch normalization is applied to

speed up convergence speed. After the convolution blocks, the features are fed into a global average pooling layer instead of a fully connected layer, reducing the number of weights. The final label is produced by a softmax layer Wang et al. (2016).

LSTM: An LSTM is a type of RNN that can learn long-term dependencies between time steps of sequential data. Contrary to CNN, an LSTM can remember the state of the network between predictions. The essential components of an LSTM network are a sequence input layer to incorporate time-series data into the network and an LSTM layer to learn long-term dependencies between time steps of sequence data. The LSTM layer contains hidden units providing inputs to memory cells and their corresponding gate units. All units (except for gate units) have connections to all units in the next layer Hochreiter & Schmidhuber (1997). In our implementation, we set the LSTM parameter n_layers in tsai Oguiza (2020) to 2.

BiLSTM: The BiLSTM network extends the traditional LSTM networks. While the LSTM layer considers the time sequence in a forward direction, the BiLSTM layer considers it both backward and forwards Graves & Schmidhuber (2005). Indeed, the BiLSTM network trains two LSTM networks on the input sequence. During this process, the first recurrent layer is replicated in the network, and therefore two layers are created side-by-side. The input sequence will be an input to the first layer; meanwhile, its reversed replica will be an input to the second layer. This approach adds additional context to the network, resulting in faster and better model learning.

LSTM-FCN & BiLSTM-FCN: It has been shown that the performance of FCN for time series classification can enhance by adding LSTM sub-modules Karim et al. (2018). The fully convolutional part of this architecture consists of three temporal convolutional blocks. Each block contains a temporal convolutional layer, accompanied by batch normalization followed by a ReLU activation function. Following the final convolution block, global average pooling is applied. In parallel, the time-series input is fed into a dimension shuffle layer. Next, the transformed time series as the output of the shuffle layer is passed into the LSTM block containing the LSTM layer, followed by a dropout. Finally, the output of the global pooling layer (from the fully convolutional part) and the LSTM block are concatenated and passed onto a softmax classification layer Karim et al. (2018).

MLSTM-FCN & MBiLSTM-FCN: MLSTM-FCN and MBiLSTM-FCN are multivariate time series classification models whose architecture is based on the univariate time series classification models, including LSTM-FCN and Attention LSTM-FCN. The fully convolutional part in both groups (i.e., univariate and multivariate time series classification models) consists of three temporal convolutional blocks. However, compared to LSTM-FCN, the first two convolutional blocks conclude with a squeeze-and-excite block that adaptively recalibrates the input feature maps. This process can be considered as a form of learned self-attention on the output feature maps of prior layers Karim et al. (2019).

ResNet: Similar to FCN, the architecture of ResNet consists of three residual blocks, followed by a global average pooling layer and a softmax layer. The presence of a shortcut connection in each residual block makes the structure of Resnet very deep and enables the gradient to flow directly through the bottom layers. The filters in both architectures of FCN and ResNet are very similar. While the convolution extracts the local features in the temporal axis, the sliding filters take into account the dependencies among different time intervals and frequencies. Compared to FCN, ResNet is claimed to be a better candidate to be applied to larger and more complex data because it is more likely to strike a good trade-off between generalization and interpretability Wang et al. (2016).

ResCNN: ResCNN is a hybrid scheme for time series classification that integrates a residual network with a CNN. In ResCNN, the strength of ResNet and CNN are combined. ResNet can learn highly complex patterns in the data due to the presence of a shortcut connection technique. However, this technique is computationally expensive and can easily cause overfitting. On the other hand, although CNN is capable of learning the temporal and spatial patterns from raw data, it cannot recover the complex patterns in the data because of few levels of the network. The architecture of ResCNN is constructed by facilitating a residual learning block at the first three convolutional layers to incorporate the strength of both networks. Additionally, batch normalization and diverse activation functions are adopted in different layers of ResCNN to enhance the nonlinear abstraction capacity.

Moreover, in order to avoid overfitting, the pooling operation is removed, and the features are fed into a global average pooling instead of a fully connected layer Zou et al. (2019).

InceptionTime: Inspired by the Inception-v4 architecture, the InceptionTime is an ensemble of 5 Inception networks, with each prediction given an even weight. Each Inception network contains only two residual blocks compare to ResNet, with three residual blocks. Each block in the inception network comprises three Inception modules rather than traditional fully convolutional layers. The first principal component of the Inception module is the "bottleneck" layer which allows the Inception network to have much longer filters than ResNet (almost ten times), with roughly the same number of parameters to be learned. The second major component of the Inception module is sliding multiple filters of different lengths simultaneously on the same input time series Fawaz et al. (2020).

XceptionTime: Inspired by InceptionTime, XceptionTime is designed to be independent of the time window. The use of adaptive average pooling in this architecture makes XceptionTime more robust to the temporal translation of the inputs as the temporal information will sum out. One key difference between the XceptionTime module and InceptionTime module previously proposed in Fawaz et al. (2020), is adopting depthwise separable convolutions, which significantly mitigates the required number of parameters in the network and also can lead to higher accuracy Rahimian et al. (2019).

XCM: Compared to typical CNN architectures, XCM extracts observed variables features (2D convolution filters) and time features (1D convolution filters) directly from the input data. Features related to time fully incorporate the timing information from the input data, not from the processed features related to observed variables (features maps from 2D convolution filters). Therefore, on average, this process can lead to a better classification performance than the 2D/1D sequential approach. XCM uses 1D global average pooling followed by a softmax layer for classification, which reduces the number of trainable parameters and improves the network's generalization ability Fauvel et al. (2020).